LOCKHEED MISSILES & SPACE COMPANY INC.

HUNTSVILLE RESEARCH & ENGINEERING CENTER

HUNTSVILLE RESEARCH PARK

4800 BRADFORD DRIVE, HUNTSVILLE, ALABAMA

BACKFLOW OF OUTGAS CONTAMINATION ONTO ORBITING SPACECRAFT AS A RESULT OF INTERMOLECULAR COLLISIONS

June 1972

Contract NAS8-26554

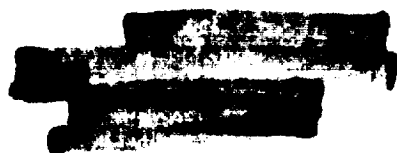by

S. J. Robertson

APPROVED: _____

B. Hobson Shirley, Supervisor
Aerophysics Section

_____

George D. Reny, Manager
Aeromechanics Dept.

_____

for J.S. Farrior
Resident Director

FOREWORD

This interim report documents the results accomplished during performance of Task A of Contract NAS8-26554, "Mass Transport Contamination Study," Modification 1. The work was performed by personnel in the Aeromechanics Department of the Lockheed-Huntsville Research & Engineering Center under Contract to NASA-Marshall Space Flight Center. The MSFC technical monitor for the contract is E.E. Klingman, S&E-SSL-PM.

Preceding page blank

ii

CONTENTS

iii

Section 1
INTRODUCTION AND SUMMARY

Orbiting space vehicles lose mass to the ambient environment as a result of outgassing of spacecraft materials, dumping of waste products and firing of attitude control reaction motors. Some of the lost mass will return to the vehicle, where even very small amounts may significantly cloud spacecraft windows, contaminate experiment packages or otherwise interfere with spacecraft operations.

In the highly rarefied environment at orbital altitudes, backscattering due to intermolecular collisions will be a primary mode by which outgas products will be deflected back onto the vehicle. The intermolecular collisions will be of two distinct types. First, they will occur between the outflowing molecules and the ambient atmospheric molecules. The stream of ambient atmospheric molecules will be highly energetic, corresponding to the orbital velocity of the spacecraft. Intermolecular collisions of this type will consequently tend to strongly deflect the outflowing molecules in the direction of the ambient freestream. Second, intermolecular collisions will occur between individual outflowing molecules because of differences in velocity (including direction) of the individual molecules.

To provide an indication of the amount of backflow to be expected, a theoretical analysis was performed based on the following simplifying assumptions. The spacecraft was assumed to be spherical in shape with the mass flow emitting uniformly over the spherical surface at a constant rate and in a D'Lambertian spatial distribution. The outflow gases were assumed to be neutrally charged and of a single species with a molecular weight characteristic of a composite of the actual species involved in the mass flow.

The theoretical analysis showed that, for outgassing only, less than 1.5% of the outgas products will return to the Skylab spacecraft as a result of inter-molecular collisions. When the total mass flow from the spacecraft, including waste dumps, reaction control motor firings, etc., was considered, it was estimated that about 30% will return to the spacecraft. The latter result is based on certain rather extreme simplifying assumptions.

Section 2

METHOD OF APPROACH AND DERIVATION OF EQUATIONS

2.1 METHOD OF APPROACH

The highly rarefied environment under consideration is such that the flow may be considered to be "nearly free molecular." In this flow regime, the mean free-path between intermolecular collisions is large compared to typical spacecraft dimensions, yet small enough to cause significant departure from free molecular flow. The fact that the flow regime is indeed nearly free molecular will be shown later for the Skylab spacecraft.

In this flow regime, the "first-collision" model approach of Baker and Charwat (Ref. 1) is appropriate. Each molecule is considered to undergo a maximum of one intermolecular collision prior to colliding with a surface, or between two successive collisions with a surface. In the present applications, this allows two classes of collisions to be considered: (1) between an outflowing molecule and an ambient atmospheric molecule, neither of which has undergone previous collisions; and (2) between two outflowing molecules which have not experienced prior collisions. Collisions between ambient atmospheric molecules are neglected altogether since the frequency of such collisions is extremely small compared to that of the other two classes of collisions. Actually, Baker and Charwat considered only class (1) collisions. Since it is difficult to show that class (2) collisions are in fact negligible (Ref. 2), they will be considered in this analysis by using certain simplifying assumptions.

The first-collision approach considers the molecules to be smooth, hard elastic spheres of some finite diameter. In the present analysis, the diameter is made flexible depending on the relative velocity between collisions to account for realistic temperature variations in viscosity.

2-1

2.2 DERIVATION OF EQUATIONS

It is necessary first to determine the collision rate per unit volume that occurs in the region surrounding the sphere. Next, a determination is made of the number of colliding outflow molecules in an element of volume which are deflected back in the direction of a given point on the surface. The total back-flow flux at the given point is then determined by integrating over the half space outward from the point on the surface. This is described separately for the two classes of collisions in the following paragraphs.

2.2.1 Scattering by Ambient Atmospheric Molecules

Consider the geometrical representation shown in Fig. 1. The point on the sphere surface at which the backflow flux is to be calculated is designated Q, while a point in the field surrounding the sphere which is a source of back-scattered molecules is designated P. For convenience Q is considered to be in the $\vec{i}$, $\vec{j}$ plane, where $\vec{i}$, $\vec{j}$ and $\vec{k}$ are unit vectors in the direction of corresponding rectangular coordinates with $\vec{i}$ pointing in the negative direction of the ambient flow. The angle ϕ is the latitudinal displacement from the $\vec{i}$ axis. In the primed coordinate system, $\vec{i}'$ is in the direction of the radius passing through Q, $\vec{j}'$ is in the $\vec{i}$, $\vec{j}$ plane and $\vec{k}'$ is in the $\vec{k}$ direction. ϕ' and θ' are polar coordinates about the $\vec{i}'$ axis. Finally, r is the distance from the sphere center out to P, while r' is the distance from Q to P.

The collision rate per unit volume, $\dot{n}$, in the field surrounding the sphere is given by:

$$\dot{n} = n_e n_\infty |\vec{V}_\infty - \vec{v}_e| \sigma_{e-\infty} \tag{1}$$

where n_e is the density field of outflow molecules, n_∞ is the density of the ambient atmosphere, $\vec{V}_\infty$ is the ambient flow velocity, $\vec{v}_e$ is the velocity of the outflow molecules and $\sigma_{e-\infty}$ is the cross section for collisions between the outflow molecules and the ambient atmospheric molecules.
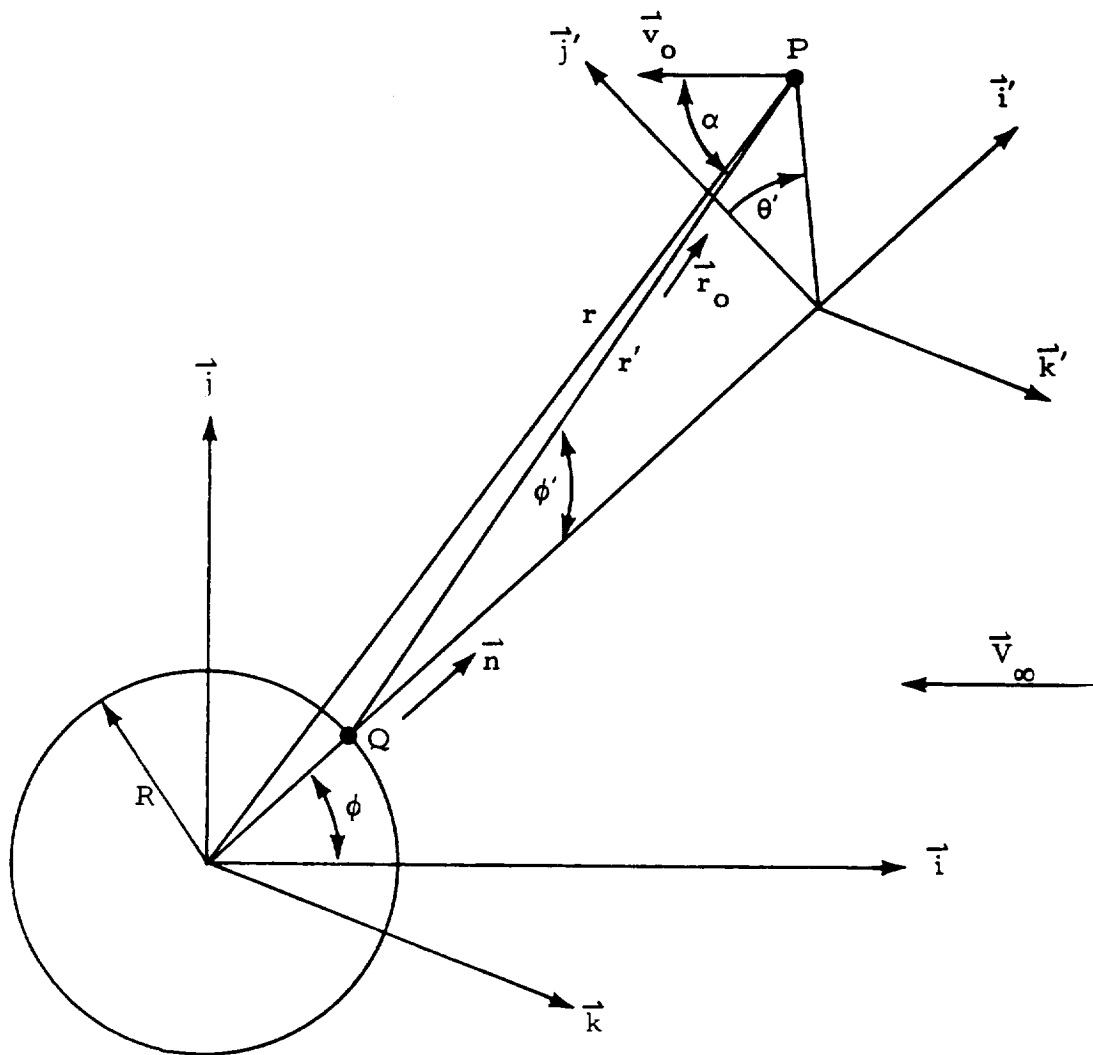
2-2

Fig. 1 - Geometrical Representation of Scattering by Ambient
Atmospheric Molecules

The density field n_e of outflowing molecules at P is determined by

$$n_e = \int_\Omega \frac{q_w}{\overline{v}_w} \frac{d\omega}{\pi} \qquad (2)$$

where q_w is the outflow flux at the sphere surface, $\overline{v}_w$ is the mean velocity of the outflow molecules and the integration is over the solid angle ω subtended by the sphere at P. We assume here that the variation in the density field is due entirely to the diverging flow away from the sphere, and that attenuation due to collisions may be neglected. This assumption is justified by the mean free-path being much larger than the sphere radius, as is shown later for the Skylab spacecraft.

Carrying out the integration in Eq. (2) yields

$$n_e = \frac{2 \, q_w}{\overline{v}_w} \frac{r - \sqrt{r^2 - R^2}}{r} \qquad (3)$$

Referring again to Eq. (1), $\dot{n}$ is seen to be given by

$$\dot{n} = \frac{2 \, q_w \, n_\infty \, |\overline{V}_\infty - \overline{v}_e| \, \sigma_{e-\infty}}{\overline{v}_w} \frac{r - \sqrt{r^2 - R^2}}{r} \qquad (4)$$

Next, the directional distribution must be determined of scattering of those outflow molecules undergoing collisions in an element of volume at P. To do this, the velocity of the outflow molecules is assumed to be negligible compared to the velocity of the ambient atmospheric molecules. The outflow molecules may then be considered stationary with respect to the sphere. Consider the hard sphere collision shown schematically in Fig. 2. For all collisions in which the line of centers is in the solid angle element $d\omega$, the stationary molecule will be deflected into $d\omega$ on the opposite side of the stationary molecule. The probability dP_ω of the line of centers lying in $d\omega$ is given by the amount of sphere surface contained in $d\omega$ projected in the direction of flow ratioed to
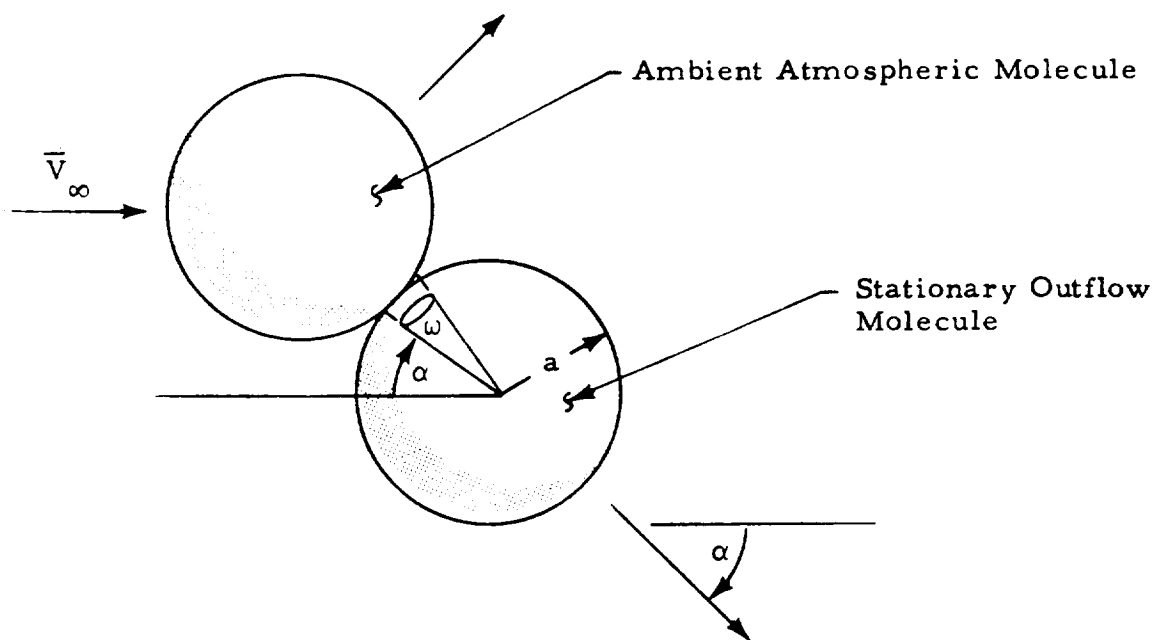
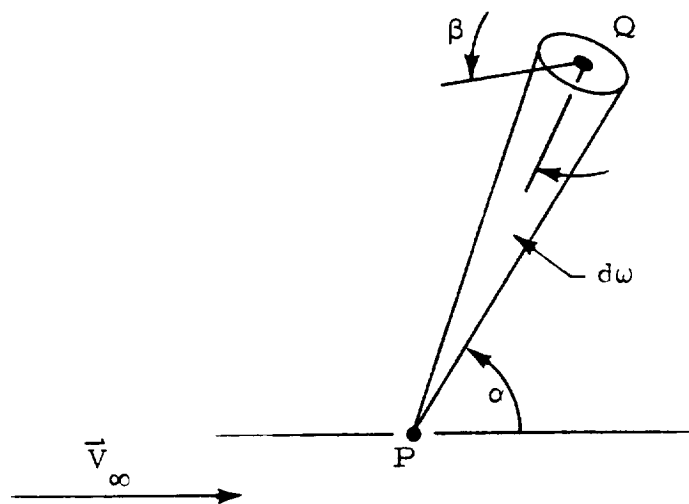Fig. 2 - Schematic of Hard Sphere Collision

Fig. 3 - Diagram for Scattered Flux Due to Collisions

the sphere cross section:

$$dP_\omega = \frac{a^2 \, d\omega}{\pi a^2} \cos\alpha = \frac{\cos\alpha}{\pi} \, d\omega \qquad (5)$$

Now, referring to Fig. 3, the flux dq_b is found of scattered outflow molecules from collisions in volume element dV at P and crossing surface element dA at Q. Surface element dA is oriented at angle β to the line joining P and Q, and Q is at a distance r' from P.

$$dq_b = \frac{\dot{n} \, dV \frac{\cos\alpha}{\pi} \, d\omega}{r'^2 \, d\omega} \cos\beta = \frac{\dot{n} \cos\alpha \cos\beta}{\pi r'^2} \, dV \qquad (6)$$

Referring again to Fig. 1, the flux dq_b of backscattered outflow molecules at Q is

$$q_b = \frac{2 \, q_w \, n_\infty \, V_\infty \, \sigma_{e-\infty}}{\pi \, \bar{v}_w} \int \frac{\cos\alpha \, \cos\phi'}{r'^2} \left(\frac{r - \sqrt{r^2 - R^2}}{r} \right) dV \qquad (7)$$

where the volumetric integral is carried out over the portion of the half space outward from dA at Q which is also forward of Q in the negative direction of the external flow (recall from Fig. 2 that molecules are scattered only in the forward direction).

Before Eq. (7) is evaluated for arbitrary ϕ, the integration is performed at $\phi = 0$ and at $\phi = \pi/2$.

$$\frac{q_{b,o}}{q_w} = \frac{4 \, n_\infty \, V_\infty \, \sigma_{e-\infty}}{\bar{v}_w} \int_o^{\pi/2} \cos^2\phi' \, \sin\phi' \int_o^\infty \left(\frac{r - \sqrt{r^2 - R^2}}{r} \right) dr' d\phi' \qquad (8)$$

The radial distance r under the r' integral sign is a function of r' and ϕ' as follows

$$r = (R^2 + 2\cos\phi' \, r' \, R + r'^2)^{1/2} \qquad (9)$$

2-6

The difficulty of performing the integration is lessened greatly by approximating the expression under the r' integral sign by the following simpler expression:

$$\frac{r - \sqrt{r^2 - R^2}}{r} \simeq \frac{1}{2}\left(\frac{R^2}{r^2} + \frac{R^6}{r^6}\right) \tag{10}$$

The close agreement between the two expressions is shown in Fig. 4.

Equation (8) now becomes

$$\frac{q_{b,o}}{q_w} = \frac{2\, n_\infty\, V_\infty\, \sigma_{e-\infty}\, R}{\overline{v}_w} \int_o^{\pi/2} \cos^2\phi'\, \sin\phi'$$

$$\times \left(\int_o^\infty \frac{d\widetilde{r}'}{1 + 2\cos\phi'\, \widetilde{r}' + \widetilde{r}'^2} + \int_o^\infty \frac{d\widetilde{r}'}{\left(1 + 2\cos\phi'\, \widetilde{r}' + \widetilde{r}'^2\right)^3}\right) d\phi' \tag{11}$$

where $\widetilde{r}' = r'/R$. The group of constant factors preceding the integral signs may be rearranged and expressed in terms of certain dimensionless parameters widely used in rarefied gas dynamics:

$$\frac{2\, n_\infty\, V_\infty\, \sigma_{e-\infty}\, R}{\overline{v}_w} = \sqrt{\frac{\pi}{2}}\, \frac{S_b}{Kn}\, \frac{\sigma_{e-\infty}}{\sigma_\infty} \tag{12}$$

where S_b is the ambient velocity ratioed to the most probable thermal velocity of the outflow molecules at the surface temperature, Kn is the ambient mean free-path ratioed to the sphere radius, and $\sigma_{e-\infty}/\sigma_\infty$ is the cross section for collisions between outflow molecules and ambient atmospheric molecules ratioed to the cross section for collisions between individual ambient atmospheric molecules.
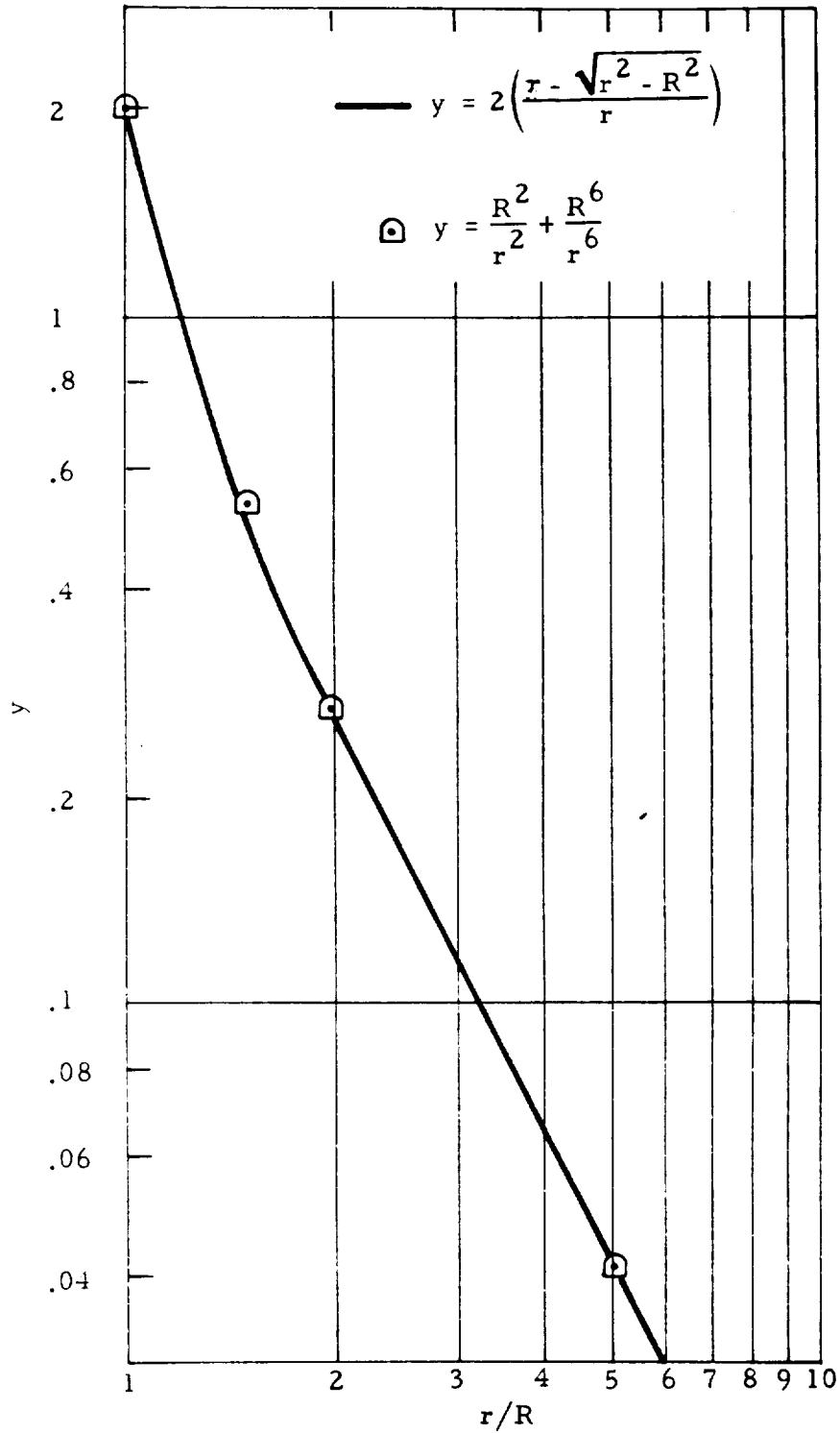
Fig. 4 - Approximate Expression $R^2/r^2 + R^6/r^6$ Compared to Exact Expression $2(r - \sqrt{r^2 - R^2})/r$

2-8

The integrals over $\tilde{r}'$ in Eq. (11) are given as follows:

$$\int_0^\infty \frac{d\tilde{r}'}{1 + 2\cos\phi\,\tilde{r}' + \tilde{r}'^2} = \frac{\phi'}{\sin\phi'} \tag{13}$$

$$\int_0^\infty \frac{d\tilde{r}'}{\left(1 + 2\cos\phi\,\tilde{r}' + \tilde{r}'^2\right)^3} = \frac{3\phi'}{8\sin^5\phi'} - \frac{\cos\phi'}{4\sin^2\phi'} - \frac{3\cos\phi'}{8\sin^4\phi'} \tag{14}$$

Equation (11) now becomes:

$$\frac{q_{b,0}}{q_w} = \sqrt{\frac{\pi}{2}}\,\frac{S_b}{Kn}\,\frac{\sigma_{e-\infty}}{\sigma_\infty}\left\{ \int_0^{\pi/2} \phi'\cos^2\phi'\,d\phi' + \frac{3}{8}\int_0^{\pi/2} \frac{\phi'\cos^2\phi'}{\sin^4\phi'}\,d\phi' \right.$$

$$\left. - \frac{1}{4}\int_0^{\pi/2} \frac{\cos^3\phi'}{\sin\phi'}\,d\phi' - \frac{3}{8}\int_0^{\pi/2} \frac{\cos^3\phi'}{\sin^3\phi'}\,d\phi' \right\}$$

$$= \frac{3\pi^2 - 8}{48}\sqrt{\frac{\pi}{2}}\,\frac{S_b}{Kn}\,\frac{\sigma_{e-\infty}}{\sigma_\infty} \tag{15}$$

For $\phi = \pi/2$, making use of the results of Eqs. (10) and (12) through (14), Eq. (7) becomes:

$$\frac{q_{b,\pi/2}}{q_w} = \frac{1}{\sqrt{2\pi}}\,\frac{S_b}{Kn}\,\frac{\sigma_{e-\infty}}{\sigma_\infty}\int_0^{\pi/2}\cos\theta\,d\theta\int_0^{\pi/2}\sin\phi'\cos\phi'$$

$$\times\left\{ \phi' + \frac{3}{8}\frac{\phi'}{\sin^4\phi'} - \frac{1}{4}\frac{\cos\phi'}{\sin\phi'} - \frac{3}{8}\frac{\cos\phi'}{\sin^3\phi'} \right\}d\phi' = \frac{5}{32}\sqrt{\frac{\pi}{2}}\,\frac{S_b}{Kn}\,\frac{\sigma_{e-\infty}}{\sigma_\infty} \tag{16}$$

or

$$\frac{q_{b,\pi/2}}{q_{b,0}} = \frac{15}{2(3\pi^2 - 8)} = 0.3471 \tag{17}$$

For general ϕ, the integration of Eq. (7) becomes much more tedius. The angle α is expressed in terms of ϕ, ϕ' and θ' as follows:

$$\alpha = \cos^{-1} (\cos\phi \cos\phi' - \sin\phi \sin\phi' \cos\theta') \qquad (18)$$

Recall that the volumetric integral in Eq. (7) is carried out over the portion of the half space forward of Q in the negative direction of the external flow. This is equivalent to requiring that $0 \le \alpha \le \pi/2$. For $0 \le \phi \le \pi/2$, Eq. (7) becomes:

$$\frac{q_b}{q_w} = \frac{1}{\sqrt{2\pi}} \frac{S_b}{Kn} \frac{\sigma_{e-\infty}}{\sigma_\infty} \left\{ \int_0^{\frac{\pi}{2}-\phi} \int_0^{\pi} (\cos\phi \cos\phi' - \sin\phi \sin\phi' \cos\theta') \cos\phi' \right.$$

$$\times \left(\phi' + \frac{3}{8} \frac{\phi'}{\sin^4\phi'} - \frac{1}{4} \frac{\cos\phi'}{\sin\phi'} - \frac{3}{8} \frac{\cos\phi'}{\sin^3\phi'}\right) d\theta' d\phi'$$

$$+ \int_{\frac{\pi}{2}-\phi}^{\pi/2} \int_{\cos^{-1}\frac{1}{\tan\phi \tan\phi'}}^{\pi} (\cos\phi \cos\phi' - \sin\phi \sin\phi' \cos\theta') \cos\phi'$$

$$\times \left. \left(\phi' + \frac{3}{8} \frac{\phi'}{\sin^4\phi'} - \frac{1}{4} \frac{\cos\phi'}{\sin\phi'} - \frac{3}{8} \frac{\cos\phi'}{\sin^3\phi'}\right) d\theta' d\phi' \right\} \qquad (19)$$

Performing the integrations over θ' reduces Eq. (19) to:

$$\frac{q_b}{q_w} = \frac{1}{\sqrt{2\pi}} \frac{S_b}{Kn} \frac{\sigma_{e-\infty}}{\sigma_\infty}$$

$$\times \left\{ \pi \cos\phi \int_0^{\pi/2} \cos^2\phi' \left(\phi' + \frac{3}{8} \frac{\phi'}{\sin^4\phi'} - \frac{1}{4} \frac{\cos\phi'}{\sin\phi'} - \frac{3}{8} \frac{\cos\phi'}{\sin^3\phi'}\right) d\phi' \right.$$

$$- \cos\phi \int_{\frac{\pi}{2}-\phi}^{\pi/2} \cos^{-1}\frac{1}{\tan\phi \tan\phi'} \cos^2\phi' \left(\phi' + \frac{3}{8} \frac{\phi'}{\sin^4\phi'} - \frac{1}{4} \frac{\cos\phi'}{\sin\phi'} - \frac{\cos\phi'}{\sin^3\phi'}\right) d\phi'$$

$$+ \cos\phi \int_{\frac{\pi}{2}-\phi}^{\pi/2} \sqrt{\tan^2\phi \, \tan^2\phi' - 1} \, \cos^2\phi' \left(\phi' + \frac{3}{8} \frac{\phi'}{\sin^4\phi'} - \frac{1}{4} \frac{\cos\phi'}{\sin\phi'} - \frac{3}{8} \frac{\cos\phi'}{\sin^3\phi'} \right) d\phi' \Bigg] \quad (20)$$

The first integral in Eq. (20) is identical to the integral in Eq. (15):

$$\int_{o}^{\pi/2} \cos^2\phi' \left(\phi' + \frac{3}{8} \frac{\phi'}{\sin^4\phi'} - \frac{1}{4} \frac{\cos\phi'}{\sin\phi'} - \frac{3}{8} \frac{\cos\phi'}{\sin^3\phi'} \right) d\phi' = \frac{3\pi^2 - 8}{48} \quad (21)$$

After some algebraic manipulation is performed, and expressing in terms of the flux at $\phi = 0$, Eq. (20) then becomes:

$$\frac{q_b}{q_{b,o}} = \left\{ \cos\phi + \frac{48}{\pi(3\pi^2 - 8)} \sin\phi \int_{\frac{\pi}{2}-\phi}^{\pi/2} \left[\sqrt{1 - \frac{\tan^2(\frac{\pi}{2} - \phi')}{\tan^2\phi}} - \frac{\tan(\frac{\pi}{2} - \phi')}{\tan\phi} \cos^{-1} \frac{\tan(\frac{\pi}{2} - \phi')}{\tan\phi} \right] \right.$$

$$\left. \times \sin\phi' \cos\phi' \left(\phi' + \frac{3}{8} \frac{\phi'}{\sin^4\phi'} - \frac{1}{4} \frac{\cos\phi'}{\sin\phi'} - \frac{3}{8} \frac{\cos\phi'}{\sin^3\phi'} \right) d\phi' \right\} \quad (22)$$

To allow integration in closed form, the first factor under the integral sign is approximated as follows:

$$\sqrt{1 - \frac{\tan^2(\frac{\pi}{2} - \phi')}{\tan^2\phi}} - \frac{\tan(\frac{\pi}{2} - \phi')}{\tan\phi} \cos^{-1} \frac{\tan(\frac{\pi}{2} - \phi')}{\tan\phi}$$

$$\simeq 1 - \frac{\pi}{2} \frac{\tan(\frac{\pi}{2} - \phi')}{\tan\phi} + (\frac{\pi}{2} - 1) \frac{\tan^2(\frac{\pi}{2} - \phi')}{\tan^2\phi} \quad (23)$$

The approximation was obtained by fitting the quadratic equation to match end points at $x = \tan(\frac{\pi}{2} - \phi')/\tan\phi' = 0$ and 1 and the first derivative at $x = 0$.

Very close agreement between the exact and approximate expressions is shown in the comparison in Fig. 5.

Equation (22) may now be expressed as follows:

$$\frac{q_b}{q_{b,o}} = \left\{ \cos\phi + \frac{48}{\pi(3\pi^2 - 8)} \left[\sin\phi \int_{\frac{\pi}{2}-\phi}^{\pi/2} \sin\phi' \cos\phi' \right.\right.$$

$$\times \left(\phi' + \frac{3}{8} \frac{\phi'}{\sin^4\phi'} - \frac{1}{4} \frac{\cos\phi'}{\sin\phi'} - \frac{3}{8} \frac{\cos\phi'}{\sin^3\phi'} \right) d\phi'$$

$$- \frac{\pi}{2} \cos\phi \int_{\frac{\pi}{2}-\phi}^{\pi/2} \cos^2\phi' \left(\phi' + \frac{3}{8} \frac{\phi'}{\sin^4\phi'} - \frac{1}{4} \frac{\cos\phi'}{\sin\phi'} - \frac{3}{8} \frac{\cos\phi'}{\sin^3\phi'} \right) d\phi'$$

$$\left.\left. + (\frac{\pi}{2} - 1) \frac{\cos^2\phi}{\sin\phi} \int_{\frac{\pi}{2}-\phi}^{\pi/2} \frac{\cos^3\phi'}{\sin\phi'} \left(\phi' + \frac{3}{8} \frac{\phi'}{\sin^4\phi'} - \frac{1}{4} \frac{\cos\phi'}{\sin\phi'} - \frac{3}{8} \frac{\cos\phi'}{\sin^3\phi'} \right) d\phi' \right] \right\} \quad (24)$$

The first integral is seen to be identical to the integral in Eq. (16) for $\phi = \pi/2$, while the other two integrals drop out due to the $\cos\phi$ factors. Also, all three integrals drop out at $\phi = 0$ due to the identity of the limits of integrations, leaving the first term equal to unity. At $\phi = 0$ and $\pi/2$, therefore, Eq. (24) reduces to the previous results for those particular points.

Carrying out the integrations in Eq. (24) yields:

$$\frac{q_b}{q_{b,o}} = \left\langle \cos\phi + \frac{48}{\pi(3\pi^2 - 8)} \left\{ \frac{\sin\phi}{2} \left[(\frac{\pi}{2} - \phi) \sin^2\phi + \phi \right. \right.$$

$$\left. - \frac{1}{8} \sin2\phi + \frac{3}{8} (\frac{\pi}{2} \tan^2\phi - \frac{\phi}{\cos^2\phi} - \tan\phi) \right]$$

$$y = \sqrt{1 - x^2} - x \cos^{-1} x$$

$$\bigcirc \quad y = 1 - \pi/2\ x + \left(\frac{\pi}{2} - 1\right) x^2$$
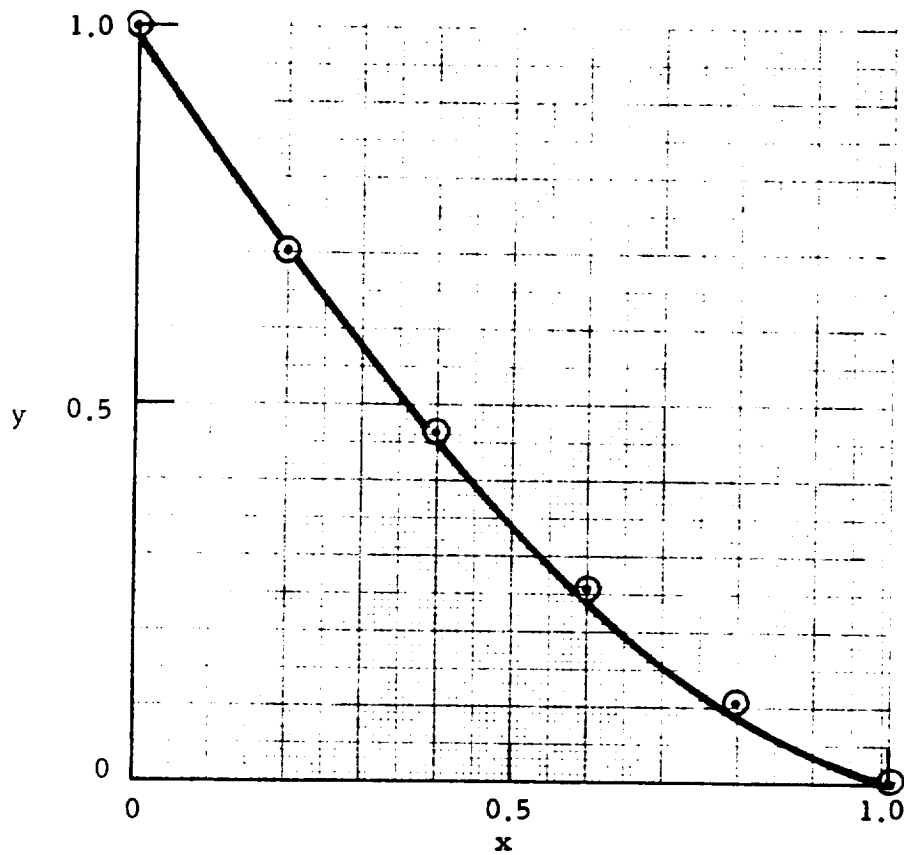

Fig. 5 - Approximate Expression $1 - \frac{\pi}{2} x + \left(\frac{\pi}{2} - 1\right) x^2$ Compared to Exact Expression $\sqrt{1 - x^2} - x \cos^{-1} x$

$$-\frac{\pi}{8}\cos\phi\left[\pi\phi - (\frac{\pi}{2} - \phi)\sin2\phi - \phi^2 - \frac{1}{2}\sin^2\phi + \frac{1}{2}\tan^2\phi\left((\frac{\pi}{2} - \phi)\tan\phi - 1\right)\right]$$

$$+ (\frac{\pi}{2} - 1)\frac{\cos^2\phi}{\sin\phi}\left[\frac{1}{32}\left(3(\frac{\pi}{2} - \phi)\tan^4\phi - 3\tan^3\phi + \tan\phi\right.\right.$$

$$\left.\left.+ 2\sin2\phi - 5\phi\right) - (\frac{\pi}{2} - \phi)\ln\cos\phi - \frac{1}{2}(\frac{\pi}{2} - \phi)\sin^2\phi - \int_0^\phi \ln\cos x\, dx\right]\Big]\Big\rangle \quad (25)$$

There remains now only the task of evaluating the integral of the lncosx. To accomplish this, lncosx is approximated as follows:

$$\ln\cos x \cong \ln\left(\frac{\frac{\pi}{2} - x}{\frac{\pi}{2}}\right) + \frac{2}{\pi}x - \frac{\pi^2 - 4}{2\pi^2}x^2 \quad (26)$$

This expression was obtained by matching the end point values and the first and second derivatives at x = 0, and requiring the limit of the ratio of the two expressions to approach unity as $x \longrightarrow \pi/2$. Good agreement is shown in the comparison of the two expressions in Fig. 6. Performing the integral yields:

$$\int_0^\phi \ln\cos x\, dx = -\frac{\pi}{2}\left[(1 - \frac{2}{\pi}\phi)\ln(1 - \frac{2}{\pi}\phi) + \frac{2}{\pi}\phi\right] + \frac{1}{\pi}\phi^2 - \frac{\pi^2 - 4}{6\pi^2}\phi^3 \quad (27)$$

Combining this result with Eq. (25) yields the final result for $0 < \phi < \pi/2$:

$$\frac{q_b}{q_{b,o}}\left\langle\cos\phi + \frac{48}{\pi(3\pi^2 - 8)}\left\{\frac{\sin\phi}{2}\left[(\frac{\pi}{2} - \phi)\sin^2\phi + \phi\right.\right.\right.$$

$$\left.\left.- \frac{1}{8}\sin2\phi + \frac{3}{8}(\frac{\pi}{2}\tan^2\phi - \frac{\phi}{\cos^2\phi} - \tan\phi)\right]\right.$$

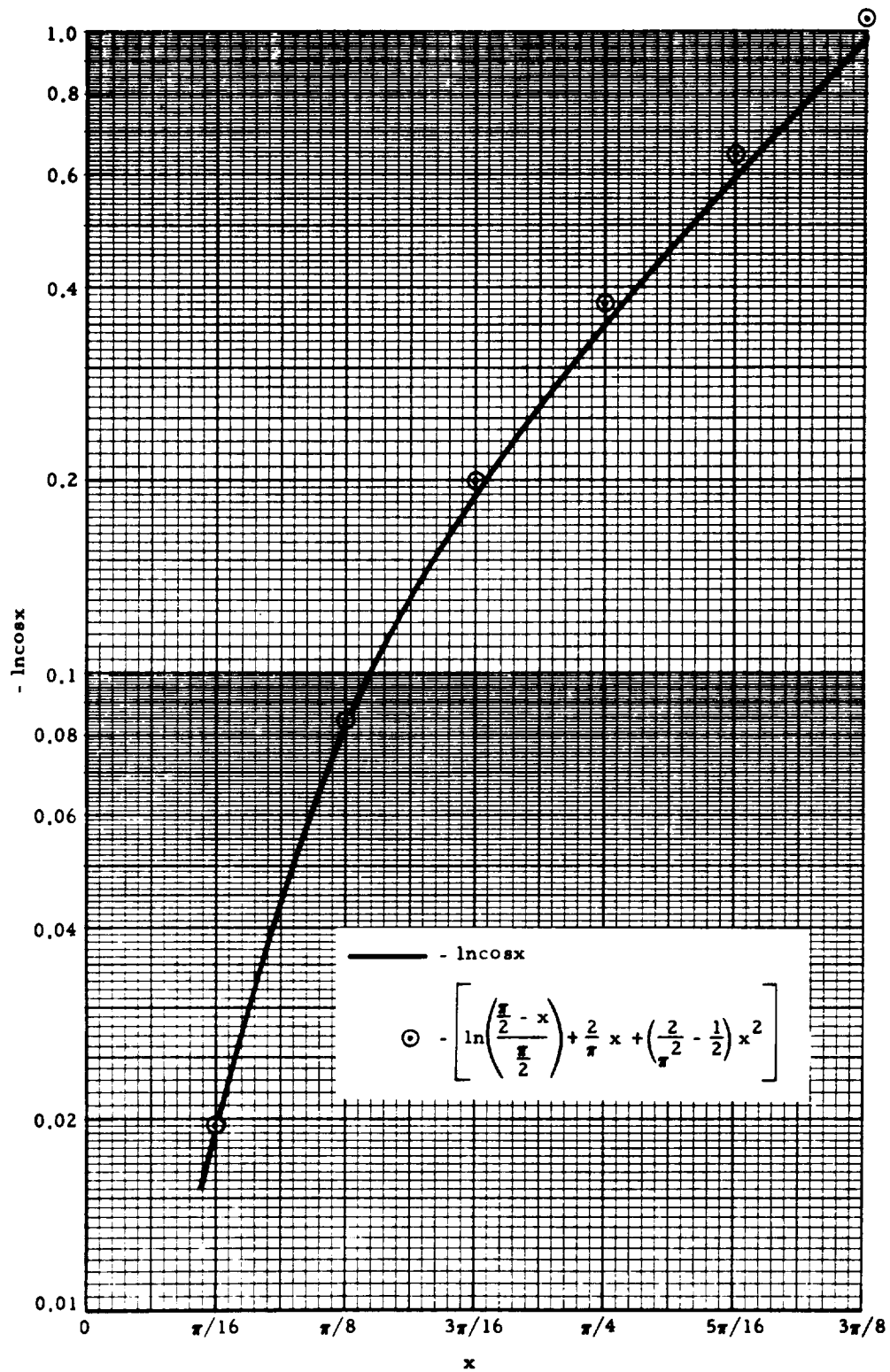$$\left.- \frac{\pi}{8}\cos\phi\left[\pi\phi - (\frac{\pi}{2} - \phi)\sin2\phi - \phi^2 - \frac{1}{2}\sin^2\phi\right.\right.$$

Fig. 6 - Comparison of Approximate and Exact Expressions for lncosx

$$+ \frac{1}{2} \tan^2\phi \left((\frac{\pi}{2} - \phi) \tan\phi - 1 \right) \right] + (\frac{\pi}{2} - 1) \frac{\cos^2\phi}{\sin\phi} \left[\frac{1}{32} \left(3(\frac{\pi}{2} - \phi) \tan^4\phi - 3\tan^3\phi + \tan\phi \right. \right.$$

$$+ 2\sin2\phi - 5\phi \right) - (\frac{\pi}{2} - \phi)\ln\cos\phi - \frac{1}{2}(\frac{\pi}{2} - \phi)\sin^2\phi + \frac{\pi}{2}\left((1 - \frac{2}{\pi}\phi)\ln(1 - \frac{2}{\pi}\phi) + \frac{2}{\pi}\phi \right)$$

$$\left. \left. - \frac{1}{\pi}\phi^2 + \frac{\pi^2 - 4}{6\pi^2}\phi^3 \right] \right] \right\rangle \tag{28}$$

For $\pi/2 < \phi < \pi$, Eq. (7) becomes

$$\frac{q_b}{q_w} = \frac{1}{\sqrt{2\pi}} \frac{S_b}{Kn} \frac{\sigma_{e-\infty}}{\sigma_\infty}$$

$$\times \left\{ -\cos\psi \int_{\pi/2-\psi}^{\pi/2} \cos^{-1}\frac{1}{\tan\psi\tan\phi'} \cos^2\phi' \left(\phi' + \frac{3}{8}\frac{\phi'}{\sin^4\phi'} - \frac{1}{4}\frac{\cos\phi'}{\sin\phi'} - \frac{3}{8}\frac{\cos\phi'}{\sin^3\phi'} \right) d\phi' \right.$$

$$\left. + \cos\psi \int_{\pi/2-\psi}^{\pi/2} \sqrt{\tan^2\psi\tan^2\phi' - 1} \cos^2\phi' \left(\phi' + \frac{3}{8}\frac{\phi'}{\sin^4\phi'} - \frac{1}{4}\frac{\cos\phi'}{\sin\phi'} - \frac{3}{8}\frac{\cos\phi'}{\sin^3\phi'} \right) d\phi' \right\} \tag{29}$$

where $\psi = \pi - \phi$. Comparing Eq. (29) to Eq. (20) reveals the two equations to be identical except for the absence in Eq. (29) of the first integral in Eq. (20), and the substitution of $\pi - \phi$ for ϕ. The results obtained for $0 < \phi < \pi/2$ can be used, therefore, to obtain results for $\pi/2 < \phi < \pi$:

$$\frac{q_{b,\phi}}{q_{b,o}} = \frac{q_{b,\pi-\phi}}{q_{b,o}} - \cos(\pi-\phi) \tag{30}$$

Note that the results for $\phi > \pi/2$ ignore the absence of scattering in the "shadowed" volume behind the sphere. This is of no real consequence,

however, since, as is shown in the following paragraph, the calculated back-scatter flux rapidly decreases as ϕ increases beyond $\pi/2$.

The variation in backscatter flux with ϕ, as determined from Eqs. (17), (28) and (30), is given in tabular form in Table 1, and graphically in Fig. 7.

Table 1

VARIATION OF BACKSCATTER FLUX WITH ANGULAR DISPLACEMENT ON SPHERE (INTERACTION WITH AMBIENT ATMOSPHERE ONLY)

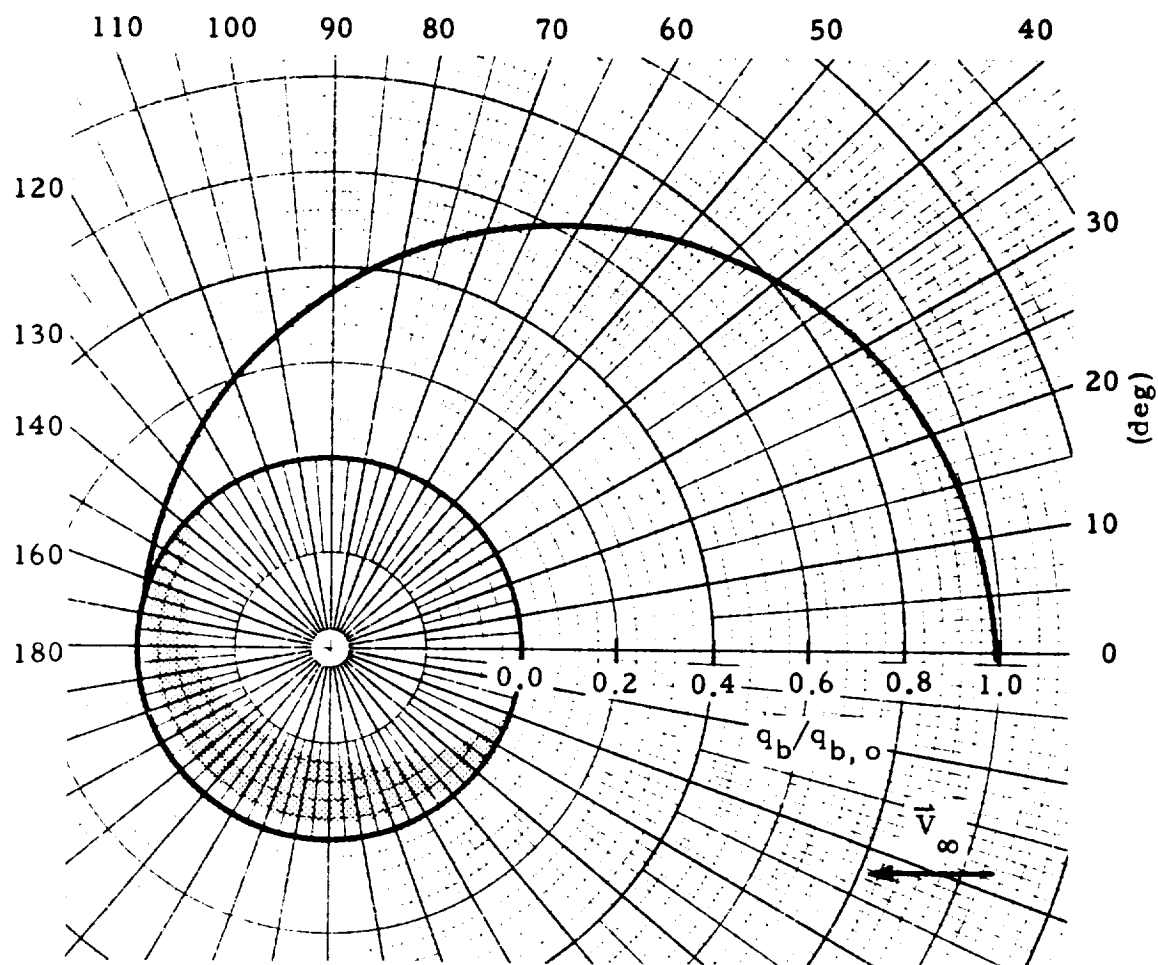| ϕ (deg)	$q_b/q_{b,o}$	ϕ (deg)	$q_b/q_{b,o}$
5	.9963	95	.3049
10	.9857	100	.2655
15	.9689	105	.2287
20	.9466	110	.1945
25	.9193	115	.1630
30	.8877	120	.1342
35	.8522	125	.1081
40	.8134	130	.0849
45	.7717	135	.0646
50	.7276	140	.0474
55	.6816	145	.0331
60	.6341	150	.0217
65	.5856	155	.0130
70	.5365	160	.0070
75	.4875	165	.0030
80	.4391	170	.0009
85	.3920	175	.0002
90	.3471	180	— 0 —

Fig. 7 - Variation of Backscatter Flux with Angular Displacement on Sphere (Interaction with Ambient Atmosphere Only)

2.2.3 Scattering Due to Collisions Between Outflow Molecules

It will be assumed for the moment that the contribution to the backscatter flux due to collisions between individual outflow molecules is small compared to that due to collisions with ambient atmospheric molecules. This assumption will be shown later to be essentially true when outgassing alone is considered. The truth of this assumption justifies the use of certain simplifying assumptions in the derivation of the backflow due to self-scattering which would otherwise be considered somewhat extreme. The assumptions will produce conservative results in that the calculated values will be greater than would be the case without the assumptions. In addition to the usual first-collision assumptions, it is assumed that the outflow molecules contained in an element of volume are composed of two groups, with the two groups traveling in opposite directions at their mean thermal velocity. The collision rate per unit volume is determined from the collisions between these two groups. In addition, it is assumed that the scattered molecules resulting from these collisions flow outward from the volume element with a spherically symmetrical directional distribution.

Based on the above assumptions, the collision rate $\dot{n}$ per unit volume is given by:

$$\dot{n} = \frac{n_e}{2} \cdot \frac{n_e}{2} \cdot (2 \bar{v}_w) \, \sigma_{e-e} \tag{31}$$

where σ_{e-e} is the cross section for collisions between outflowing molecules. Making use of Eqs. (3) and (10) yields:

$$\dot{n} = \frac{2 \, q_w^2 \, \sigma_{e-e}}{\bar{v}_w} \left(\frac{R^2}{r^2} + \frac{R^6}{r^6} \right)^2 \tag{32}$$

Now, referring again to Fig. 3, the flux $d\,q_b$ of backscattered molecules from collisions in volume element dV at P and crossing surface element dA at Q is

$$d\,q_b = \frac{\dot{n} \, \cos\beta}{4 \, \pi \, r'^2} \tag{33}$$

2-19

Using Eq. (32) and integrating over the entire half-space outward from dA at a point Q on the sphere surface (refer again to Fig. 1) yields:

$$\frac{q_b}{q_w} = \frac{q_w \, \sigma_{e-e} \, R}{\bar{v}_w} \int_0^{\pi/2} \sin\phi' \, \cos\phi' \left\{ \int_0^\infty \frac{d\tilde{r}'}{\left(1 + 2\cos\phi' \, \tilde{r}' + \tilde{r}'^2\right)^2} \right.$$

$$\left. + 2 \int_0^\infty \frac{d\tilde{r}'}{\left(1 + 2\cos\phi' \, \tilde{r}' + \tilde{r}'^2\right)^4} + \int_0^\infty \frac{d\tilde{r}'}{\left(1 + 2\cos\phi' \, \tilde{r}' + \tilde{r}'^2\right)^6} \right\} d\phi' \qquad (34)$$

The grouping of parameters preceding the integral sign in Eq. (34) may be considered an inverse Knudsen number characteristic of self-scattering:

$$\frac{q_w \, \sigma_{e-e} \, R}{\bar{v}_w} = Kn_{e-e}^{-1} \qquad (35)$$

The integrals over $\tilde{r}'$ in Eq. (34) are as follows:

$$\int_0^\infty \frac{d\tilde{r}'}{\left(1 + 2\cos\phi' \, \tilde{r}' + \tilde{r}'^2\right)^2} = \frac{1}{2} \frac{\phi'}{\sin^3\phi'} - \frac{1}{2} \frac{\cos\phi'}{\sin^2\phi'} \qquad (36)$$

$$\int_0^\infty \frac{d\tilde{r}'}{\left(1 + 2\cos\phi' \, \tilde{r}' + \tilde{r}'^2\right)^4} = \frac{5}{16} \frac{\phi'}{\sin^7\phi'} - \frac{5}{24} \frac{\cos\phi'}{\sin^4\phi'} - \frac{5}{16} \frac{\cos\phi'}{\sin^6\phi'} - \frac{1}{6} \frac{\cos\phi'}{\sin^2\phi'} \qquad (37)$$

$$\int_0^\infty \frac{d\tilde{r}'}{\left(1 + 2\cos\phi' \, \tilde{r}' + \tilde{r}'^2\right)^6} = \frac{63}{256} \frac{\phi'}{\sin^{11}\phi'} - \frac{63}{384} \frac{\cos\phi'}{\sin^8\phi'} - \frac{63}{256} \frac{\cos\phi'}{\sin^{10}\phi'}$$

$$- \frac{21}{160} \frac{\cos\phi'}{\sin^6\phi'} - \frac{9}{80} \frac{\cos\phi'}{\sin^4\phi'} - \frac{1}{10} \frac{\cos\phi'}{\sin^2\phi'} \qquad (38)$$

Using Eqs. (36) through (38), Eq. (34) now becomes

$$
\frac{q_b}{q_w} = Kn_{e-e}^{-1} \left\{ \frac{1}{2} \int_0^{\pi/2} \phi' \frac{\cos\phi'}{\sin^2\phi'} d\phi' - \frac{1}{2} \int_0^{\pi/2} \frac{\cos^2\phi'}{\sin\phi'} d\phi' \right.
$$

$$
+ \frac{5}{8} \int_0^{\pi/2} \phi' \frac{\cos\phi'}{\sin^6\phi'} d\phi' - \frac{5}{12} \int_0^{\pi/2} \frac{\cos^2\phi'}{\sin^3\phi'} d\phi' - \frac{5}{8} \int_0^{\pi/2} \frac{\cos^2\phi'}{\sin^5\phi'} d\phi'
$$

$$
- \frac{1}{3} \int_0^{\pi/2} \frac{\cos^2\phi'}{\sin\phi'} d\phi' + \frac{63}{256} \int_0^{\pi/2} \phi' \frac{\cos\phi'}{\sin^{10}\phi'} d\phi' - \frac{63}{384} \int_0^{\pi/2} \frac{\cos^2\phi'}{\sin^7\phi'} d\phi'
$$

$$
- \frac{63}{256} \int_0^{\pi/2} \frac{\cos^2\phi'}{\sin^9\phi'} d\phi' - \frac{21}{160} \int_0^{\pi/2} \frac{\cos^2\phi'}{\sin^5\phi'} d\phi' - \frac{9}{80} \int_0^{\pi/2} \frac{\cos^2\phi'}{\sin^3\phi'} d\phi'
$$

$$
\left. - \frac{1}{10} \int_0^{\pi/2} \frac{\cos^2\phi'}{\sin\phi'} d\phi' \right\}
\tag{39}
$$

Carrying out all of the integrals in Eq. (39) would be extremely laborious and, considering the assumptions involved in the derivation of this equation, rather unprofitable. For this reason, only the first term within the brackets in Eq. (34), and, hence, the first two terms in Eq. (39), will be retained in the following development. Carrying out the integration of these terms yields

$$
\frac{q_b}{q_w} = \frac{4-\pi}{4} Kn_{e-e}^{-1}
\tag{40}
$$

Section 3
APPLICATION TO SKYLAB SPACECRAFT

A typical configuration of the Skylab spacecraft, with the Apollo Telescope Mount (ATM), is shown in Fig. 8. An equivalent size sphere would be roughly 15 to 20 m in diameter. For purposes of this analysis, an equivalent diameter of 20 m (or a radius of 10 m) is assumed.

The operating altitude of the Skylab spacecraft is 435 kilometers. At this altitude, the ambient mean free path is 1.38×10^4 m (Ref. 3), and the circular orbit velocity is 7640 m/sec. The spacecraft surface temperature will vary widely, ranging between about 235 and 380°K, depending upon position in orbit and other parameters. Assuming a surface temperature of 300°K and a molecular weight of 24, the most probable thermal velocity of the outflowing molecules is 456 m/sec. Based on the above data, the ambient Knudsen number, Kn, is 691 and the speed ratio S_b is 16.7.

The collision cross section $\sigma_{e-\infty}$ will vary depending on the relative velocity between the colliding particles. This variance is reflected in the temperature variation of viscosity. For hard sphere molecules, the viscosity is proportional to the square root of temperature and inversely proportional to the cross section (Ref. 4). Conversely, the effective cross section may be considered proportional to the square root of temperature and inversely proportional to viscosity. This is expressed as follows:

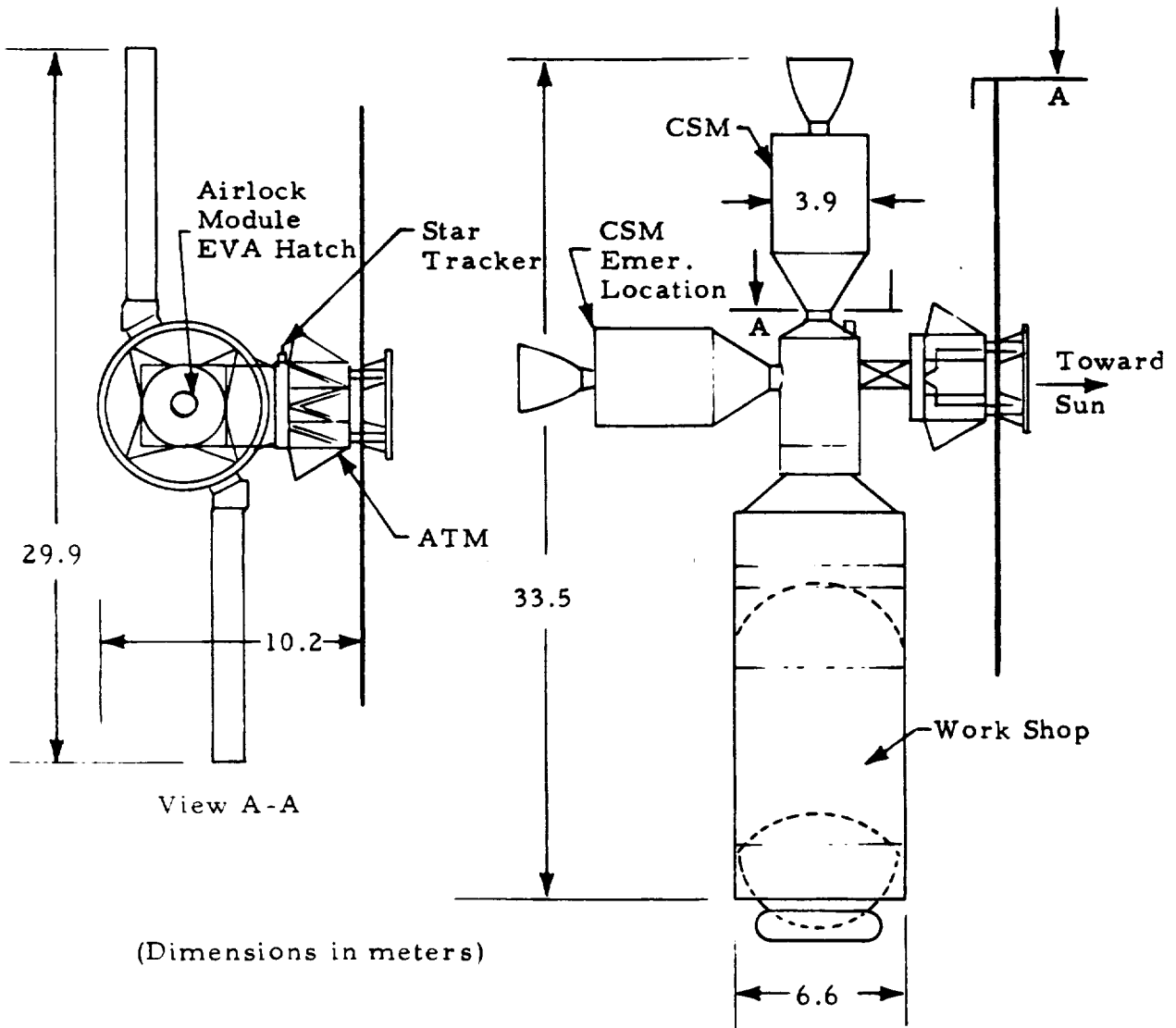$$\frac{\sigma_{e-\infty}}{\sigma^*} = \left(\frac{\bar{T}_{e-\infty}}{T^*} \right)^{-(n-\frac{1}{2})} \tag{41}$$

3-1

Fig. 8 - Schematic of Typical Configuration of Skylab Spacecraft Showing Approximate External Dimensions

where $\overline{T}_{e-\infty}$ is an effective temperature corresponding to the relative velocity between colliding molecules, σ^* is the viscosity at a reference temperature T*, and n is the exponent in the power-law variation of viscosity with temperature. Based on molecular data in Ref. 4, a value of 43.0×10^{-16} cm^2 for σ^* at temperature $T^* = 300°K$ is assumed, and a value 0.8 for the exponent n. From atmospheric data in Ref. 3, $\sigma_\infty = 41.9 \times 10^{-16}$ cm^2. The effective temperature $\overline{T}_{e-\infty}$ can be defined in a number of ways, all of which should be based on a proportionality with the square of the relative velocity. We will define it as follows:

$$\overline{T}_{e-\infty} = \frac{1}{3} \frac{\overline{M}}{R_g} V_\infty^2 \tag{42}$$

where $\overline{M}$ is the average molecular weight of the colliding molecules and R_g is the universal gas constant. This expression is based on the mean-square velocity relationship to temperature for a Maxwellian gas. $\overline{T}_{e-\infty}$ is thus found to be $50,200°K$. Based on the above data, the cross section ratio $\sigma_{e-\infty}/\sigma_\infty$ is found to be 0.22.

Using the values which were obtained for Kn, S_b and $\sigma_{e-\infty}/\sigma_\infty$, the dimensionless factor defined by Eq. (12) is found to be 0.00665. This factor may be considered an inverse Knudsen number $Kn_{e-\infty}^{-1} = R/\lambda_{e-\infty}$ characteristic of collisions between outflowing and ambient molecules. The characteristic mean-free-path $\lambda_{e-\infty}$ is seen to be much greater than the sphere radius, thus justifying the assumption of nearly free molecular flow.

Using the above results and Eq. (15), the backscatter flux at $\phi = 0$, due to interaction with the ambient atmosphere, is now found to be 0.003, or 0.3%, of the outgas rate. If the collision cross section had been considered constant and unaffected by the relative velocity, the cross section ratio $\sigma_{e-\infty}/\sigma_\infty = \sigma^*/\sigma_\infty = 1.13$, and the resulting backscatter flux would be 1.5% of the outgas rate.

LOCKHEED - HUNTSVILLE RESEARCH & ENGINEERING CENTER

From Eqs. (35) and (40) it is seen that the fractional intensity of back-flow due to self-scattering is dependent on the outgas rate. First, assume an outgas rate based on an estimated 30 kg/day total weight loss rate for the Skylab spacecraft. Based on the 10 m radius for the equivalent sphere, this amounts to an outgas rate of 2.77×10^{-8} g/cm^2/sec. Recall that this quantity includes waste dumps, attitude control reaction motor firings, etc., in addition to outgassing. This assumed value is actually about three orders of magnitude greater than that which could be expected for simple outgassing.

From Eq. (35), the inverse Knudsen number Kn_{e-e}^{-1} for self-scattering is found to be 1.39. The characteristic mean-free-path, therefore, is about 0.67 of the sphere radius. This mean-free-path value is of marginally satis-factory magnitude for the first-collision assumptions used in the analysis. From Eq. (40), the backscatter flux due to self-scattering is found to be 0.30, or 30%, of the outgas rate. This value is quite large, and, in view of the lumping together of such contributions as waste dumps and reaction motor firings, the question arises as to the validity of the results.

Waste dumps and reaction motor firings occur itermittently and at rather high instantaneous pressures compared to the average, assuming a continuous discharge. The flow regime, therefore, is actually much more nearly continuum than free molecular, and the mass flow returning to the vehicle is more likely due to direct jet impingement than to intermolecular collisions.

A typical outgas rate for spacecraft materials is 3.9×10^{-11} g/cm^2/sec for BBRC "one" paint, air dried (Ref. 5). For this outgas rate, and still assuming M = 24, Kn_{e-e}^{-1} is 2.4×10^{-3}. The mean-free-path is now about 400 times the sphere radius. This is well within the nearly free molecular flow regime. From Eq. (40) the backscatter flux due to self-scattering is found to be 0.0005, or 0.05%, of the outgas rate.

Section 4
CONCLUDING REMARKS

The derivation of equations in this study is fairly rigorous for back-flow due to interaction with the ambient atmosphere. Some rather extreme simplifying assumptions were made, however, for the case of self-scattering. When outgassing alone is considered, the contribution to backflow due to self-scattering is found to be fairly small, about an order of magnitude smaller than that due to interaction with the ambient atmosphere. The rather extreme simplifying assumptions for self-scattering, therefore, are found to be justified.

When all forms of mass flow from the spacecraft, including waste dumps, reaction motor firings, etc., are averaged together into a single continuous out-flow rate, the density of this averaged outflow is sufficiently high that self-scattering is found to far overshadow interactions with the ambient atmosphere. The simplifications made in the analysis of self-scattering, therefore, greatly reduce the accuracy of the calculated backflow. Also, as was pointed out in the preceding section, the primary mode of backflow onto the spacecraft from waste dumps and reaction motor firings is probably direct jet impingement rather than intermolecular collisions.

Considering outgassing alone, only a small fraction, $1\frac{1}{2}\%$ at most, of the outgas products return to the spacecraft as a result of intermolecular collisions. For some outgas products, even this small amount may significantly contaminate sensitive experiment packages. Considering the total outflow (waste dumps, reaction motor firings, etc.), a rather large fraction, about 30%, was estimated to return to the spacecraft. This is certainly a significant quantity; however, questions of accuracy of the analysis, and even its applicability to waste dumps and jets, should be considered in evaluating the results.

4-1

Section 5

REFERENCES

1. Baker, R. M. L., Jr., and A. F. Charwat, "Transitional Correction to the Drag of a Sphere in Free Molecule Flow," Phys. Fluids, Vol. 1, March-April 1958, p. 73.

2. Willis, D. R., "A Study of Near-Free Molecule Flow," in PROJECT RAND, Aerodynamics of the Upper Atmosphere (compiled by D. J. Masson), R-339, The Rand Corporation, Santa Monica, Calif., 8-10 June 1959.

3. "U. S. Standard Atmosphere, 1962," Superintendent of Documents, U. S. Government Printing Office, Washington, D. C., December 1962.

4. Kennard, E. H., Kinetic Theory of Gases, McGraw-Hill, New York, 1938.

5. Shrodt, J., "ATM Contamination Follow-On Study," Vol. II, TN 67-68, Ball Brothers Research Corporation, Boulder, Colo., 28 October 1967.